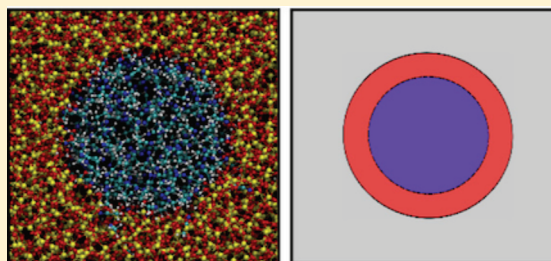


Structure and Dynamics of Acetonitrile Confined in a Silica Nanopore

Liwen Cheng, Joseph A. Morrone, and B. J. Berne*

Department of Chemistry, Columbia University, 3000 Broadway, MC 3103, New York, New York 10027, United States

ABSTRACT: Acetonitrile confined in silica nanopores with surfaces of varying functionality is studied by means of molecular dynamics simulation. The hydrogen-bonding interaction between the surface and the liquid is parametrized by means of first-principles molecular dynamics simulations. It is found that acetonitrile orders into bilayer like structures near the surface, in agreement with prior simulations and experiments. A newly developed method is applied to calculate relevant time correlation functions for molecules in different layers of the pore. This method takes into account the short lifetimes of the molecules in the layers. We compare this method with prior techniques that do not take this lifetime into account and discuss their pitfalls. We show that in agreement with experiment, the dynamics of the system may be described by a two population model that accounts for bulk-like relaxation in the center and frustrated dynamics near the surface of the pore. Specific hydrogen-bonding interactions are found to play a large role in engendering this behavior.



1. INTRODUCTION

The study of liquids confined or near an interface is an area of active experimental and computational investigation. The properties of liquids under these conditions can be very different from those in the bulk. In the present study, we consider the impact of confinement on acetonitrile. Acetonitrile (CH_3CN) is a polar, aprotic, linear molecule with amphiphilic character in the sense that the cyanide end is capable of accepting hydrogen bonds, whereas the methyl group has hydrophobic character. Experiments have been performed to elucidate the behavior of acetonitrile at the silica interface.^{1,2} The resulting picture gleaned from optical Kerr effect (OKE) spectroscopy¹ is that the liquid is ordered at the interface in successive layers pointing in opposite directions, with the closest layer to the surface effectively anchored by hydrogen-bonding interactions. This latter point is indicated by the relatively slow reorientational relaxation of molecules near the surface. The experimental data are well fit based on the assumption that there are two populations, a dynamically frustrated surface population and a population that exhibits bulk-like relaxation times in the center of the pore.

Several recent theoretical studies^{3–6} have complemented the experimental work. These studies have employed potentials describing the acetonitrile–silica interactions based on combining rules that were not optimized by further fitting to experimental or ab initio data. Despite this, several aspects of the simulations are in general agreement with the picture provided by experiment.¹ On the basis of their computational study, Morales et al.^{3,4} argue that the ordering of acetonitrile near the surface is mainly due to the surface charge distribution and not the explicit hydrogen bonding of silanols to acetonitrile.

This study revisits the problem of acetonitrile confined in silica nanopores. We utilize a force field that is parametrized to yield good agreement with first-principles computations,

particularly in terms of the hydrogen-bonding interactions between silanol groups at the surface and the acetonitrile. This force field is then utilized in extensive molecular dynamics simulations to study acetonitrile confined in a nanopore. To assess the importance of explicit hydrogen bonding and surface charge, we additionally perform simulations where silanols are replaced by methyl groups as well as simulations in which the H site is eliminated and its charge is “absorbed” into the oxygen site of the OH group.³ In agreement with ref 3, we find that the observed long-range order can be explained by nonspecific electrostatic interactions. However, we find that hydrogen bonding is essential to describe the slow relaxation associated with the first layers of acetonitrile at the surface. More generally, we show that the reorientational and diffusional dynamics of acetonitrile near the interface is significantly frustrated by surface interactions. The relaxation near the surface speeds up when hydrogen-bonding interactions are muted, and it increases further when the magnitude of the surface charge distribution is lowered by methylation of the silanol groups. This picture is consonant with a recent study by Milischuk and Ladanyi,⁷ which reported frustrated dynamics for water near the silica surface and bulk-like dynamics in the center region for water confined in a silica pore. Furthermore, we find that a two-population model is a reasonable description of reorientational dynamics, in agreement with experiment.¹

To investigate the dynamics, we extend a recently developed method⁸ to calculate relevant time correlation functions for molecules in different layers of the pore. This method takes into account the short lifetimes of the molecules in the layers, whereas in a recent study⁷ the approach adopted includes contributions from molecules that can exchange between layers.

Received: January 31, 2012

Revised: March 30, 2012

Published: April 4, 2012

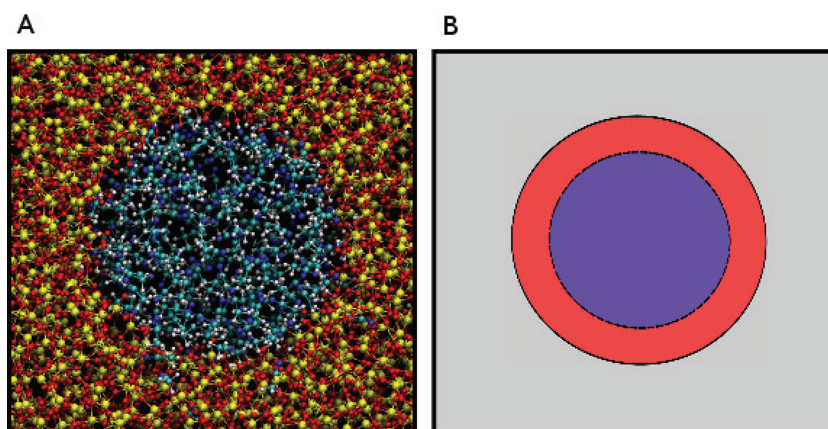


Figure 1. (A) A snapshot of the silica pore of diameter 24 Å filled with acetonitrile, taken looking down the axis of the cylindrical pore. (B) A schematic representation of the division of the acetonitrile into two populations. Red indicates the surface population, and blue indicates the center population.

This can lead to qualitative and quantitative errors when the lifetimes in any layer of interest are short. Comparing and contrasting our method with this previous method, we find that it gives an improved analysis of the spatial dependence of the dynamics.

We also investigate how the size of the pore affects the fluid structure and dynamics. Comparison of the properties of acetonitrile confined in two different sized hydroxylated silica pores of diameters 24 and 44 Å reveals that the time scale of singlet reorientational dynamics of acetonitrile in different layers is insensitive to the diameter of the pore, a result consistent with the OKE study,¹ but the angular distribution in the center of the small pore is not uniform, whereas in the larger pore it is uniform.

This Article is organized as follows: Section 2 presents the details of the simulation, whereas sections 3.1 and 3.2 present the results for the equilibrium and dynamical properties of acetonitrile confined in silica nanopores of diameters 24 and 44 Å. We also compare the properties of acetonitrile in two hydroxylated pores of different diameters. Section 4 compares our newly developed method for the dynamical properties with a previous technique. In the Appendix, we outline the development of the specialized force field utilized in this study.

2. SYSTEM DETAILS/SETUP

The force field described in the Appendix has been parametrized to agree with a first-principles simulation and has then been utilized to perform large-scale molecular dynamics simulations of the structure and dynamics of acetonitrile confined in silica nanopores. This work was performed using the GROMACS simulation package.⁹ We focus on acetonitrile molecules confined to a 24 Å diameter silica nanopore, but also compare this system to one with a pore diameter of 44 Å. The diameter of 24 Å was chosen to match the average value studied in the OKE experiment¹ and other simulation work.^{3,4} A β -cristobalite crystal in a periodic cubic box of length 57.28 Å was melted at 8000 K. After annealing from 8000 to 300 K, the amorphous silica structure was obtained. The nanopore was created by cutting a cylindrical hole out of the amorphous silica. This generates under-coordinated silicon and oxygen sites at the surface. The surface was functionalized with silanols by saturating the under-coordinated silicon with hydroxyl groups and the under-coordinated oxygens with hydrogen atoms, while keeping the whole system electrically neutral. The density of

silanols at the surface is approximately 4.5 per nm², which is in agreement with the 2–6 per nm² range in experiments depending on the thermal history of the sample.^{1,10} The empty pore was then filled with 280 acetonitrile molecules. The number of acetonitrile molecules in the pore was determined by running an isothermal–isobaric ensemble (NPT) simulation where the pore is in a reservoir of acetonitriles at 1 atm and 300 K, following the procedure in Rodriguez et al.'s work.¹¹ In prior studies, the density of acetonitrile in the pore has been calculated using grand canonical Monte Carlo.^{3,4,7} Our NPT simulations in liquid reservoir should predict similar densities as the grand canonical Monte Carlo simulation, provided, as is presently the case, that the height of the cylindrical pore and the thickness of the reservoir are sufficiently large. The final system contains 3319 silicon atoms, 6842 oxygen atoms, 122 silanol groups(SiOH), 21 disilanol groups(Si(OH)₂), and 280 acetonitrile molecules. A snapshot of the system is shown in Figure 1A. This system is equilibrated at 300 K in canonical ensemble (NVT) simulation for 500 ps. Starting from the positions and velocities in the equilibrated configuration, a production run was performed in the microcanonical ensemble (NVE) for 5 ns. The temperature was found to be 300 K in the NVE production run. The trajectory was saved every 100 fs.

In addition to the hydroxylated surfaces, simulations where the OH groups are replaced by methyl groups were performed. Unlike the case of the silanols, the interaction of acetonitrile with the methyl groups was garnered from combination rules and not from extensive reparameterization. Finally, to study how the removal of explicit surface hydrogen bonds affects the dynamics of liquid acetonitrile, we simulate the silanol system where each silanol hydrogen site was eliminated and its charge was “absorbed” into the O of the OH site.³ We refer to each model as OH, CH₃, and O, respectively. The number of acetonitrile molecules were found to be 235 and 262, in the CH₃ and O models, respectively. A separate simulation for bulk acetonitrile was also performed in the NVE ensemble, after setting the proper density in the NPT ensemble at 1 atm and 300 K. The bulk density was found to be 0.722 g/cm³ in the NPT simulation. The density in the center region of the pore was 0.673, 0.691, and 0.704 g/cm³ for the OH, CH₃, and O models, respectively. The somewhat lower density in the center region than in bulk was also observed in grand canonical Monte Carlo simulations for water confined in silica nanopores.⁷

In addition, we have simulated the properties of a larger hydroxylated silica pore of diameter 44 Å using the same procedure to obtain insight into the dependence of structural and dynamical properties on nanopore size. The system for this larger pore contains 5251 silicon atoms, 11 018 oxygen atoms, 288 silanol groups, 84 disilanol groups, and 1085 acetonitrile molecules in a cubic cell of length 71.6 Å. The density of silanols at the pore surface is about 4.6 per nm². The density of acetonitrile in the center region of the pore is 0.682 g/cm³.

3. RESULTS

3.1. Equilibrium. The orientational profile of the acetonitrile molecules as a function of the distance from the center of the pore is shown in Figure 2. This property is

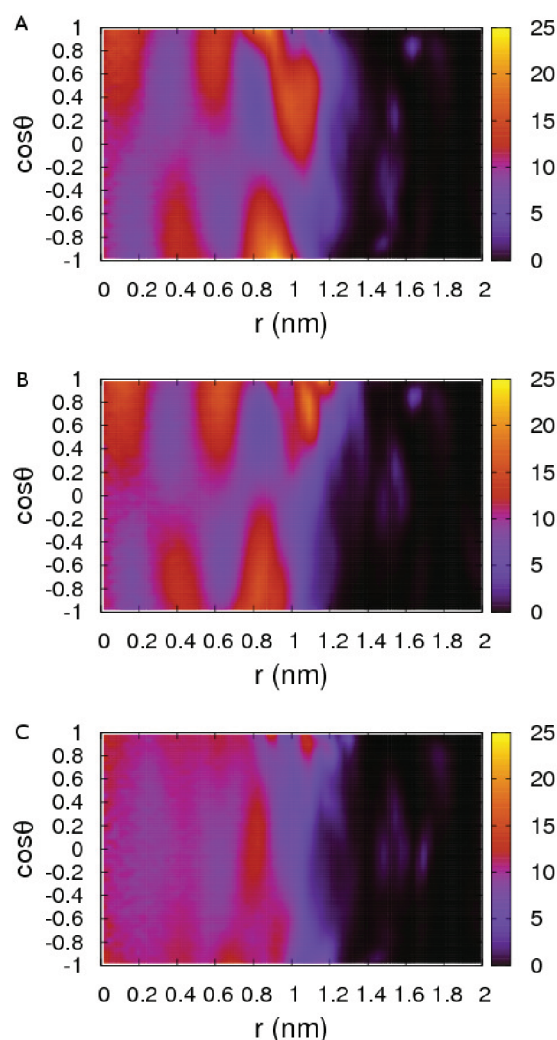


Figure 2. The orientational density distribution $F(r, \cos \theta)$ as defined in the text. Panels A, B, and C depict the distribution computed from the OH, O, and CH3 pores of diameter 24 Å, respectively.

computed as follows. Cylindrical coordinates, (r_i^{com}, z_i) , are utilized to describe the position of the center of mass of the i th acetonitrile molecule in the silica pore, and to define u_i as the unit vector pointing from the C atom to the N atom in the CN group of the i th acetonitrile molecule. Next, $(u_i \cdot r_i^{\text{com}}) = \cos \theta_i$, has a positive value when the nitrogen atom of the CN group is pointing toward the silica surface. The quantity calculated in Figure 2 is the two-dimensional histogram corresponding to the

normalized orientational density $F(r, \cos \theta) = (1/(2\pi r)) \langle (1/(N)) \sum_{i=1}^N \delta(\cos \theta - \cos \theta_i) \delta(r - \|r_i^{\text{com}}\|) \rangle$. From the orientational distribution, one can develop a clear picture of the structure of acetonitrile in the silica pore. The ordering and layering of acetonitrile is present in both the hydrogen-bonded (OH) and the non-hydrogen-bonded (O) cases. The acetonitrile molecules closest to the surface form a sublayer ($0.95 \text{ nm} < R < 1.20 \text{ nm}$), with their nitrogen atom pointing toward the surface. The acetonitrile molecules form a second sublayer ($0.75 \text{ nm} < R < 0.95 \text{ nm}$) that is oriented antiparallel to the first sublayer, with their methyl end pointing toward the surface. Antiparallel pairings are also found in the bulk acetonitrile,¹² although they possess transient lifetimes. At hydrophilic surfaces, the attraction of the first sublayer to the surface further orders the pairings in the second sublayer. This antiparallel bilayer picture has been postulated in previous studies based on optical Kerr experiments,¹ vibrational sum frequency generation experiments,⁶ and has been observed in recent simulations.^{3,5,6} The antiparallel bilayer structure also occurs in propionitrile proximate to a flat hydroxylated silica surface.¹³ Essentially the same picture is found in the present simulation. The antiparallel layering effect is still observable in the center of the pore for the OH case and the O case. However, the antiparallel bilayer ordering is not present near the methylated surface (CH3). Instead, acetonitrile molecules lie parallel to the surface when it is close to the methylated surface.

In comparison, according to Milischuk and Ladanyi, water is weakly ordered near the hydroxylated silica surface, and the ordering does not propagate further into the water as does the ordering of acetonitrile.⁷ Acetonitrile can only act as an acceptor when it makes a hydrogen bond with a silanol group, while water can act as both an acceptor and a donor. Thus, near the surface, the nitrogen end of the acetonitrile is strongly preferred by the silanol groups, while the oxygen and the hydrogen sites of water are both preferred by the silanol groups. In addition, water can form tetrahedral networks, while acetonitrile exhibits dipole pairing that is more unidirectional, and this surface templated ordering is not observed in water.

To better understand the origin of the antiparallel bilayer ordering, the charge density profiles of acetonitrile and silica surface are calculated as a function of the distance from the center of the pore. From the results shown in Figure 3, it can be seen that there is a significant surface dipole on the functionalized surface in both the OH and the O cases. Such surface charge distributions induce the antiparallel dipole pairing and layering of the acetonitrile. In contrast, for the methylated case, the surface charge is much smaller, and thus the ordering of the acetonitrile is significantly muted. Both the OH surface and the O surface exhibit similar long-range electrostatic effects on acetonitrile; this is in agreement with the work of Morales et al.,³ where it was found that the structure and orientation of acetonitrile in the pore are insensitive to specific hydrogen-bonding interactions. As one might expect, differences in the structure and orientation of the acetonitrile molecules nearest to the surface depend on whether or not the surface forms hydrogen bonds with acetonitrile. The radial density functions between the atoms on the acetonitrile molecules and the silanol oxygen atoms are shown in Figure 4 for the OH surface and the O surface, respectively. Here, NZ, CT, and CZ designate the nitrogen atom, the methyl carbon atom, and the cyanide carbon atom of the acetonitrile molecule, respectively. OH designates the oxygen atom of the hydroxyl

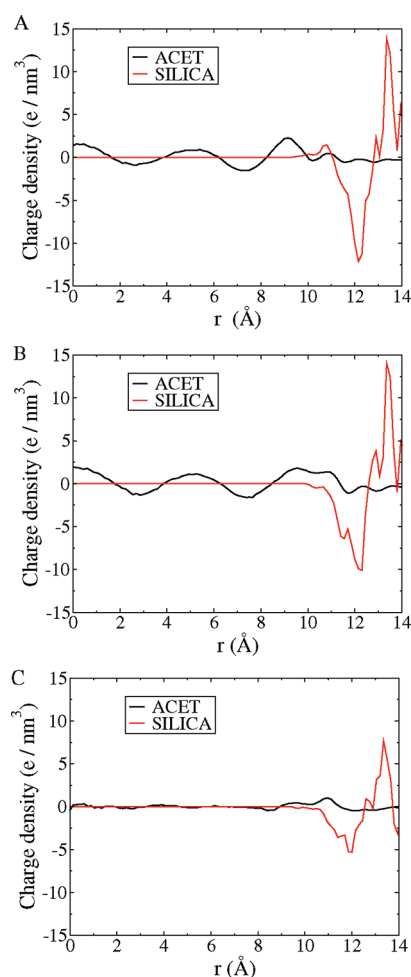


Figure 3. The charge density of acetonitrile (black curve) and silica (red curve) plotted as a function of the radial distance from the center of the silica pore of diameter 24 Å. Panels A, B, and C depict the results for the OH, O, and CH₃ systems, respectively.

group on silica surfaces. The radial distribution functions have been properly renormalized utilizing the method of Soper et al.^{14,15} to account for the excluded volume effect of the confined geometry. The nitrogen peak is much higher, and its position is closer to the oxygen in the OH case. One can see that the acetonitrile molecules near the silanol groups are more structured in the presence of hydrogen bonding. Also, it can be seen in Figure 2 that the acetonitrile molecule in the nearest sublayer to the surface points almost perpendicular to the surface with its nitrogen end toward the O-functionalized silica pore, but it is more tilted in the OH functionalized pore. This is consistent with the “bent” geometry necessitated by the formation of a hydrogen bond in the OH case. As will be shown in section 3.2, specific hydrogen-bonding interactions have a greater impact on dynamical properties.

In addition, we have attempted to compute the contact angle of acetonitrile with the flat hydroxylated and methylated silica surface. This work was prompted by recent experimental measurements of the contact angle for acetonitrile across numerous modified silica interfaces.² These experiments found that acetonitrile forms relatively low contact angles with the surface and show only slight dependence on the functionalization. According to the experiments, the contact angle of acetonitrile on the methylated silica surface is 12°; however, the

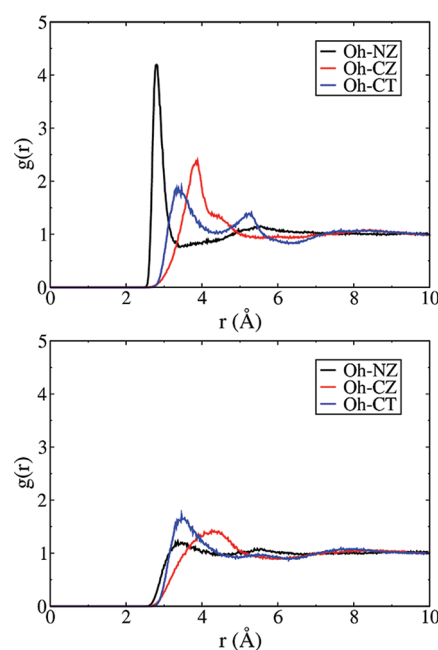


Figure 4. The radial distribution function (RDF) of various species in the OH (top panel) and O (bottom panel) pores of diameter 24 Å. The black line is the RDF between the oxygen atoms of silanols and the nitrogen atoms of acetonitrile. The red line is the RDF between the oxygen atoms of silanols and the cyanide carbon atoms of acetonitrile. The blue line is the RDF between the oxygen atoms of silanols and the methyl carbon atoms of acetonitrile.

contact angle of water on the same surface is 96°. The methylated surface is hydrophobic in water because the interactions between water molecules are strong enough that water molecules prefer to associate rather than be next to the methylated surface. In contrast, the methylated surface is not solvophobic in acetonitrile because acetonitrile molecules are amphiphilic and their interaction with each other is not significantly stronger than their interactions with the methylated surface. This difference in self-association is also reflected in the fact that the surface tension of acetonitrile is about 2.5 times smaller than the surface tension of water.¹⁶ Because of the affinity between acetonitrile and silica surfaces, all of the differently functionalized surfaces are almost entirely wetted by acetonitrile in our simulations, and the contact angle is too small to be determined without ambiguity.

Figure 5 depicts the orientational density distribution $F(r, \cos \theta)$ of acetonitrile in the hydroxylated pore of diameter 44 Å. As in the hydroxylated pore of diameter 24 Å, an antiparallel

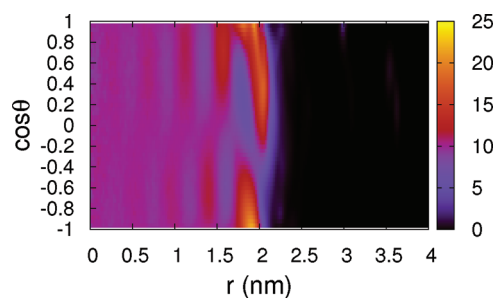


Figure 5. The orientational density distribution $F(r, \cos \theta)$ as defined in the text for the acetonitrile in the hydroxylated silica pore of diameter 44 Å.

bilayer structure is formed near the surface ($1.7 \text{ nm} < R < 2.15 \text{ nm}$). The antiparallel layering can propagate into the acetonitrile for at least 1.75 nm ($0.4 \text{ nm} < R < 2.15 \text{ nm}$), and there is still some trace of layering in the very center of the pore ($R < 0.4 \text{ nm}$). This is consistent with the finding in Hu et al.'s work⁵ that antiparallel layering effects can propagate for 2 nm in acetonitrile near a flat hydroxylated crystal surface silica.

The charge density profiles of acetonitrile in the two hydroxylated pores of different sizes are compared in Figure 6.

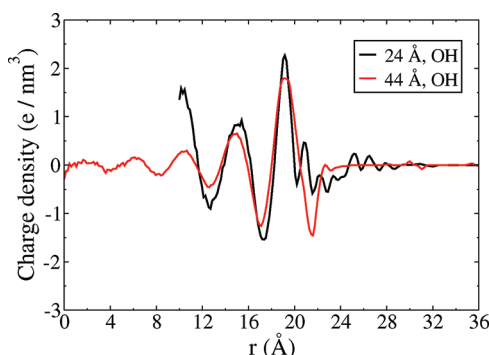


Figure 6. The charge density of acetonitrile in two hydroxylated silica pores of diameters 24 and 44 Å. The red curve is for the 44 Å pore. The black curve for the 24 Å pore has been shifted to the right by 10 Å to better compare the behavior at the silica–acetonitrile interface.

The data for the 24 Å pore have been shifted to the right by 10 Å. The positions and intensities of the charge density oscillations are similar for the first two cycles away from the surfaces in the two different pores. Yet at the third peak position, which also corresponds to the center of the pore of diameter 24 Å, the charge density in the 24 Å pore is more than 3 times that in the 44 Å pore. This enhanced density signifies that there is an in-phase construction between layering induced by the two symmetrical sides of the pore of diameter 24 Å. Such in-phase construction or out-of-phase destruction could manifest in the pores of small sizes, because the layering does not phase out in the center of small pores.

3.2. Dynamics. Experimental studies using the OKE¹ and NMR¹⁷ techniques show that the dynamics of acetonitrile near the pore surface is frustrated compared to its bulk-like behavior near the pore center. While geometrical confinement effects provide the main contribution to the frustrated dynamics of weakly wetting liquids,¹⁸ the attractive interactions with the pore surfaces largely give rise to the frustrated dynamics of strongly wetting liquids.^{1,19} We find that specific hydrogen bonding plays a dominant role in engendering the frustrated dynamics of acetonitrile in the silica pore functionalized with silanol groups, particularly with respect to orientational relaxation. The distinctive dynamics of acetonitrile near the OH pore wall and in the pore center make it necessary to use a two population exchange model to explain the total singlet reorientational dynamics. Our picture of the reorientational dynamics of acetonitrile in silica pores is consistent with the conclusions garnered from OKE experiments.^{1,19} However, it should be noted that the OKE signal is related to the time autocorrelation function of the anisotropic collective polarizability. Presently, we only consider singlet correlation functions, which do not probe the couplings between polarizability tensors in the two populations.

The singlet reorientational time correlation functions are calculated separately for the center and surface populations of acetonitrile. The surface population contains acetonitrile molecules in the two antiparallel sublayers near the silica surface (the rightmost two sublayers as shown in Figure 2A), and the center population contains acetonitrile molecules far from the surface (the leftmost three sublayers in Figure 2A). This division between the two populations is also shown in Figure 1B. Because the two populations exchange with each other by self-diffusion, it is necessary to include the survival probabilities for each population in the calculation of their reorientational correlation functions. The prescription for calculating population specific singlet time correlation functions has already been presented⁸ and is expressed in the following equation:

$$C_1(t) = \frac{1}{T} \sum_{t_0=1}^T \frac{1}{N(t_0, t_0 + t)} \sum_{i \in S(t_0, t_0 + t)} \mathbf{u}_i(t_0) \cdot \mathbf{u}_i(t_0 + t) \quad (1)$$

where $S(t_0, t_0 + t)$ is the set of molecules that stay in the layer continuously from time t_0 to $t_0 + t$, $N(t_0, t_0 + t)$ is the number of molecules in the set $S(t_0, t_0 + t)$, and \mathbf{u}_i is a unit vector pointing from the nitrogen atom to the methyl carbon atom on the i th molecule. We note that in previous simulation studies: (a) either the dynamic properties were reported for the total population,³ (b) the population specific dynamic properties were calculated in a way that neglects the exchange between different regions,⁷ or (c) the properties were reported only for molecules that stayed in a prescribed region for a time equal to the maximum correlation time computed.^{5,6} Approach (b) can cause problems when the exchange between different populations is faster than the decay of the time correlation functions being calculated. Approach (c) yields error bars that grow larger even at very short times as the maximum correlation time studied is increased, because the population averaged over will become vanishingly small.

The results calculated for the three different systems are shown in Figure 7A. The time correlation function (TCF) $C_1(t)$ for bulk acetonitrile is also shown. Unlike bulk acetonitrile, the TCFs of acetonitrile in the three pore systems decay to nonzero plateaus, no matter whether they are for the surface populations or the center populations. However, we observe that when the silica surface is made purely repulsive, the TCFs (not shown) in the two populations both decay to zero. The difference lies in the ordering and layering effect by the somewhat rugged silica surface and the surface heterogeneity shown in our small system size. The acetonitrile molecules in the surface population are ordered by their interaction with the silica surface. Although the surface layer has approximate cylindrical symmetry, the probability that one acetonitrile can change its orientation significantly by moving along the surface without leaving the surface layer is small, so that to relax their orientations such molecules must exchange with populations that are further away than the correlation length of orientational pair correlations. Thus, in the pores we observe a plateau at long times in the TCFs for the surface population. The TCFs for the center populations in the three models are very similar to each other; however, they also decay to a plateau (of value 0.11), which is smaller than is found for the surface population, either because the pore radius is not large as compared to the above-mentioned correlation length, or more likely because our constructed heterogeneous silica

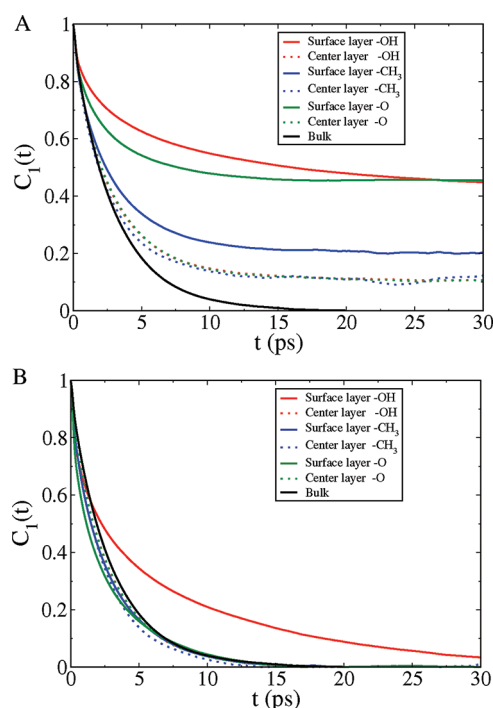


Figure 7. (A) The singlet reorientational time correlation function of acetonitrile in different regions in the OH, CH₃, and O of diameter 24 Å. (B) The time correlation function of the fluctuations in the singlet orientation obtained by first subtracting the plateau value, and then renormalization of the results shown in panel A. The red, blue, and green colors indicate the OH, CH₃, and O pores, respectively. The solid and dotted lines are for the surface population and the center population, respectively. Black indicates the behavior of bulk acetonitrile.

surfaces happen to have unbalanced charge distributions in the Y direction. As a result, the acetonitrile has an average preferential orientation in the Y direction ($\langle u_Y \rangle = 0.3$). Below, we show that the plateaus for the center populations disappear for larger pores sizes.

The plateau values in the TCFs for the surface populations of the OH and O models are much greater than for the CH₃ model, where the ordering of acetonitrile is muted. The much less frustrated dynamics in the CH₃ model demonstrate that the attractive interactions with the pore surfaces dominate the frustrated dynamics of strongly wetting liquids. Loughnane et al. also made this point based on the faster reorientational decay observed in OKE experiments when they methylated the silanol groups on the pore surfaces.^{1,19} Moreover, hydrogen-bonding interactions give rise to the frustrated short and intermediate time orientational relaxation. This is not so obvious in Figure 7A, as the long time plateau values are different. To make this point clearer, the TCFs of the fluctuations in the singlet orientation are obtained by renormalization of the $C_1(t)$ after subtracting the corresponding long time plateau values. From the results shown in Figure 7B, the relaxation of the fluctuations in the singlet orientation is greatly retarded and nonexponential only in the surface population of the OH system where the hydrogen bonding is present. The relaxation in other populations is close to the exponential relaxation of the bulk. The bulk relaxation can be fit by an exponential function $\exp(-t/\tau_b)$ with $\tau_b = 2.87$ ps. The relaxation in the surface population of the OH model can be fit by a stretched exponential function $\exp(-t/\tau)^\alpha$ with $\tau = 4.41$

ps and $\alpha = 0.577$. Although the structures of liquid acetonitrile are similar for the OH and O systems, the relaxation decays of the surface populations for these two systems are quite different, as is indicated in Figure 7B. This finding underlines the indispensable role that hydrogen-bonding interactions play in governing the dynamical properties acetonitrile near the hydroxylated surface.

Loughnane et al. proposed a two-population exchange model for the collective reorientation dynamics of acetonitrile confined in hydroxylated nanoporous glasses.¹ In their model, acetonitrile molecules in silica pores partition into two distinct populations with different reorientation time scales, the bulk-like center population and the retarded surface population. The exchange between two populations provides the surface population another channel for reorientational relaxation. In our simulation, we find, as described above, the existence of two populations with different reorientational dynamics. The exchange between two populations can be well described via the survival probabilities in different regions. On the basis of the work of Loughnane et al., we can reconstruct the TCF of the total population in our OH pore with three functions, the population specific TCFs of the two populations (see above) and the survival probability of the surface population. Our approximate formula for the total TCF $C_{1T}(t)$ is:

$$C_{1T}(t) = \chi_c C_{1C}(t) + \chi_s S(t) C_{1S}(t) + \chi_s (1 - S(t)) C_{1C}(t) \quad (2)$$

where $C_{1C}(t)$ and $C_{1S}(t)$ are the TCFs of the center population and surface population, respectively, $S(t)$ is the survival probability of acetonitrile in the surface population, χ_c is the fraction of molecules in the center population, and $\chi_s = 1 - \chi_c$ is the fraction of molecules in the surface population. χ_c was found to be 0.405 from our simulation data by counting numbers of molecules, while Loughnane et al. found this parameter to be 0.39 at 309 K by fitting their model to optical Kerr spectroscopy data.¹ As noted in previous sections, the diameter of our pore is the same as the average value in Loughnane et al.'s work.¹ The boundaries of our surface population were determined from the density profile of acetonitrile and were set to contain the acetonitrile molecules in the two antiparallel sublayers. The thickness of the surface layer was found to be 4.5 Å in our case, while this value derived from Loughnane and co-workers' model of OKE data is 4.7 Å.¹ The first term in eq 2 accounts for the reorientation of the molecules that are initially in the center population, and we assume that the initial orientation of these molecules has been fully relaxed before they enter the surface population. The second term accounts for the reorientation of the retarded molecules that stay continuously in the surface population from time 0 to t . The third term accounts for the process by which some of the retarded molecules initially in the surface population can reorient further by exchanging with the center population. The total TCF $C_{1T}(t)$ approaches the plateau value 0.11 after 100 ps, which is also the plateau value of $C_{1C}(t)$. The total TCF can be fit by the function $A + (1 - A) \exp(-(t/\tau)^\alpha)$ with $A = 0.114$, $\tau = 4.87$ ps, and $\alpha = 0.517$. The approximated total TCF from our two-population model was compared to the total TCF calculated by definition in Figure 8. The small difference between the two shows us that the two-population model is successful at describing singlet reorientational dynamics of acetonitrile confined in the hydroxylated silica pore. Our molecular dynamics simulation provides the first support for Loughnane et al.'s two-population exchange model¹

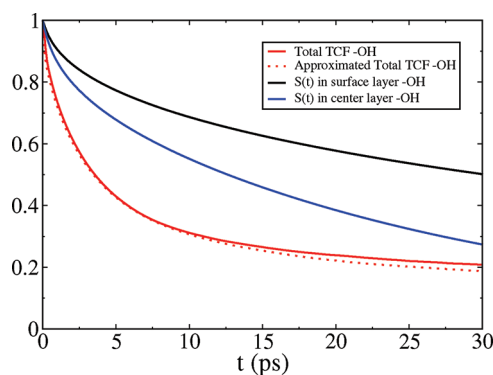


Figure 8. The singlet reorientational time correlation function of the total population in the OH pore of diameter 24 Å as calculated by definition (red solid line) and approximated by our two-population model (red dotted line). The survival probabilities of acetonitrile in the surface population (black line) and the center population (blue line) of the OH pore of diameter 24 Å.

from molecular simulation. We note that a recent computational study of water confined in a silica nanopore employed a core/shell model where the exchange between the two populations is not considered.²⁰ In agreement with the conclusions of the present work, this study found that the total second singlet reorientational TCF, $C_2(t)$, can be fit by a weighted average of the contributions from the two populations.

The translational diffusion constant has not been reported in simulation studies of acetonitrile near silica interfaces or in silica nanopores.^{3,5,6} To study the diffusion parallel to the axis of the cylindrical pore (Z axis) in the surface population and the center population, the mean square displacement is calculated from the following expression:⁸

$$\text{MSD}_{1Z}(t) = \frac{1}{T} \sum_{t_0=1}^T \frac{1}{N(t_0, t_0 + t)} \sum_{i \in S(t_0, t_0 + t)} (Z_i(t_0 + t) - Z_i(t_0))^2 \quad (3)$$

where $N(t_0, t_0 + t)$ and $S(t_0, t_0 + t)$ share the same meaning as those in eq 1. The results for our three systems are plotted in double logarithmic scale in Figure 9. Mean square displacements taking into account the survival probability have been

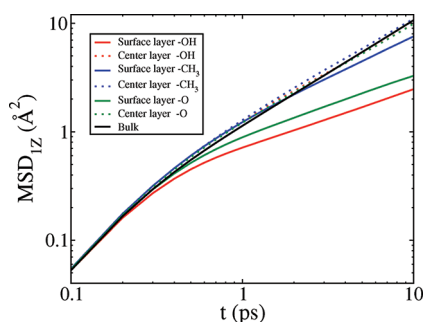


Figure 9. The mean square displacements of acetonitrile in different regions in the OH, CH₃, and O pores of diameter 24 Å. The red, blue, and green colors are for the OH, CH₃, and O pores, respectively. The solid and dotted lines are for the surface population and the center population, respectively. Black indicates the behavior of the bulk acetonitrile.

used to compute the diffusion constant parallel to the water–vapor interface in Liu et al.'s work.⁸ For times greater than 1 ps, the MSDs in the center populations enter the Brownian diffusion regime, and they are very close to the MSD in the bulk system. In contrast, the MSDs in the surface populations exhibit subdiffusive behavior for times greater than 1 ps. The subdiffusive MSDs could be fit by a power-law relationship $\text{MSD}_{1Z} = (2K_\alpha/\Gamma(1 + \alpha))t^\alpha$ derived from fractional diffusion equation²¹ with α being 0.55, 0.55, and 0.76 for the OH, O, and CH₃ models, respectively. $\Gamma(z)$ is the gamma function $\Gamma(z) = \int_0^\infty t^{z-1} e^{-t} dt$. The generalized diffusion coefficients K_α are $0.309 \text{ Å}^2/\text{ps}^{0.55}$, $0.413 \text{ Å}^2/\text{ps}^{0.55}$, and $0.605 \text{ Å}^2/\text{ps}^{0.76}$ for the OH, O, and CH₃ systems, respectively. Unlike the water–vapor interface in Liu et al.'s work,⁸ the acetonitrile molecules in our case are attracted to specific sites on the rough and heterogeneous acetonitrile–silica interfaces. The subdiffusive behavior could emerge when an acetonitrile travels on such a complex energy landscape on the surface, just like the subdiffusion found in experiments when colloidal tracer particle travels in F-actin networks.²² The sublinear power-law relationship in similar systems was also found in Rodriguez et al.'s work¹¹ where they studied the dynamics of the acetonitrile component of acetonitrile–water mixture in silica nanopores, and in Gallo et al.'s work^{23,24} where water confined in silica nanopores was studied. The mean square displacement in the bulk system shown in Figure 9 gives the diffusion constant $D_{\text{bulk}} = 0.528 \text{ Å}^2/\text{ps}$, while the value reported in one experiment study was $0.434 \text{ Å}^2/\text{ps}$.²⁵ In center populations of our three models, diffusion constants parallel to the Z axis are within a 10% range of the bulk value.

The diffusional behavior of the surface population is described by two constants, K_α and α , instead of by the one coefficient needed for the bulk liquid. Diffusion in the surface populations can be compared qualitatively by direct comparison of the magnitude of the MSDs at 10 ps instead of by comparing the values of $(K_\alpha\alpha)$ alone. As we see in Figure 9, diffusion along the Z direction of acetonitrile molecules near the surface is slowed significantly in the OH and O systems and is roughly 80% slower than in the bulk liquid, while the same motion is slowed by only 35% in the surface population of the CH₃ system. This shows that hydrophilic surfaces can strongly hinder the translational motion of acetonitrile in the two antiparallel sublayers next to the surfaces. This hindrance is reduced greatly at less attractive hydrophobic surfaces.

The dynamical properties of acetonitrile in the two different sized hydroxylated pores are compared in Figure 10. The singlet orientational TCFs and the MSDs calculated by our survival probability method are almost the same for the surface population in the two pores. As expected, surface heterogeneity has a smaller effect in the larger pore because part of the center population is further from the surface. Thus, the TCF for the center population decays to zero instead of approaching the 0.11 plateau. However, the TCFs for the center populations would be nearly the same if the 0.11 plateau is subtracted from the smaller pore's TCF, and the result is renormalized. The diffusion constant of the center population in the axial direction is $0.585 \text{ Å}^2/\text{ps}$ for the larger pore, which is greater than the $0.470 \text{ Å}^2/\text{ps}$ value for the smaller pore. This is because the center population in the larger pore contains more acetonitriles that are less influenced by the propagating layering effect. The center population in the smaller pore contains three sublayers that are still ordered considerably by the propagating layering effect. Besides these sublayers, the center population in the

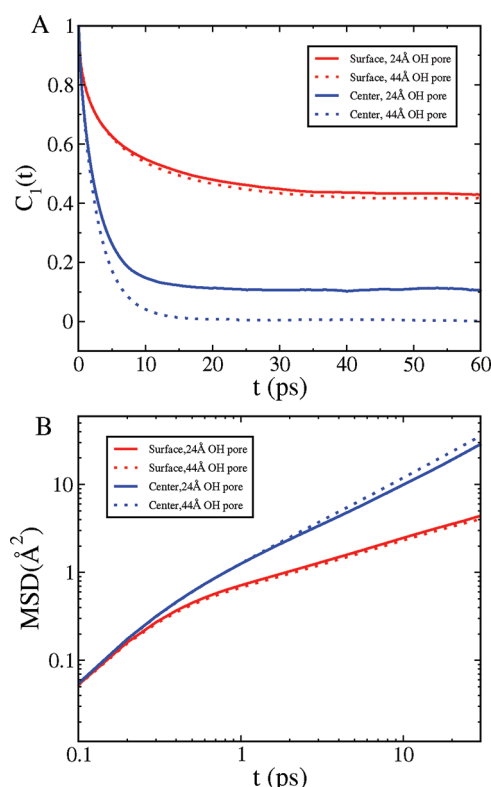


Figure 10. The dynamical properties of acetonitrile in two hydroxylated pores of diameters 24 and 44 Å calculated by the survival probability method. Panel A depicts the singlet reorientational time correlation functions in the surface population and the center population. Panel B shows the mean square displacements in the surface population and the center population. The red and blue curves depict the surface population and the center population, respectively. The solid and dotted lines indicate the 24 Å pore and the 44 Å pore, respectively.

larger pore contains five more sublayers that are weakly ordered. If we only include the molecules in the three more ordered sublayers of the center population in the larger pore, then the diffusion constant for this population is $0.500 \text{ Å}^2/\text{ps}$, which is closer to the $0.470 \text{ Å}^2/\text{ps}$ value for the smaller pore.

We also tested the two-population model for the total reorientational TCF in the larger pore. The fraction of molecules in the center population χ_c changes to 0.60. This parameter was found to be 0.61 in the OKE experiments for the hydroxylated silica pore of diameter 44 Å at 309 K.¹ The three functions used in the construction of the total TCF are shown in Figure 11. As shown in Figure 11, the total TCF constructed by this model is very close to the total TCF calculated by definition.

From the above comparisons, we conclude that the population specific dynamical properties of acetonitrile have little dependence on the size of the pore, except for the diffusion of the center population in the axial direction. This conclusion may not hold for very small pore sizes of 10 Å. For the hydroxylated pores of diameter 44 Å, the observed faster reorientational dynamics of the total population is mainly due to the larger fraction of molecules in the center population, and not from changes in the reorientational dynamics in each separate population (surface and center). In Loughnane et al.'s experimental study,¹ the OKE data were fit by a sum of three exponentials. It was found that the fitted time constants are the

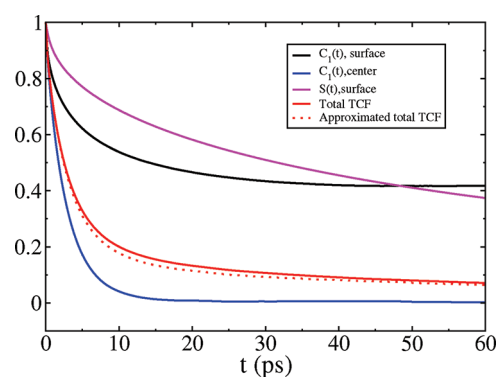


Figure 11. The singlet reorientational time correlation function of the total population for the acetonitrile in the hydroxylated pore of diameter 44 Å as calculated by definition (red solid line), and approximated by our two-population model (red dotted line). Also shown are the three functions used in the two-population model: the survival probability of acetonitrile in the surface population (magenta line), the singlet reorientational time correlation functions for the surface population (black line), and the center population (blue line) calculated by the survival probability method.

same for two different sized hydroxylated silica pores. Our conclusion is consistent with this finding.

4. COMPARISON OF TWO ANALYSIS METHODS

In a previous study of the population specific dynamical properties,⁷ molecules are considered to belong to one population for all times if their initial positions were in the specific region at a reference time. In this way, the population specific singlet orientational TCF is calculated by the following equation:

$$C^*_1(t) = \frac{1}{T} \sum_{t_0=1}^T \frac{1}{N^*(t_0)} \sum_{i \in S^*(t_0)} \mathbf{u}_i(t_0) \cdot \mathbf{u}_i(t_0 + t) \quad (4)$$

where $S^*(t_0)$ is the set of molecules that were in the specific region at a reference time t_0 , and $N^*(t_0)$ is the number of molecules in the set $S^*(t_0)$.

The TCFs calculated by this initial position method and our survival probability method for the 24 Å OH pore are shown in Figure 12A. The survival probabilities of the surface population and the center population are also shown. Although the methods yield similar results near $t = 0$, for intermediate times, the surface population TCF calculated by the initial position method decays faster than the one calculated by the survival probability method. Unlike the TCF computed by the survival probability method, it does not plateau on the intermediate time scale. Instead, at long times, it approaches the same plateau value as the TCF of the center population (not shown in figure). Clearly, the TCF for the surface population in the initial position method is actually a mixing of the TCFs for the surface population and the center population in the survival probability method, because the decay of the survival probability and the reorientation of the acetonitrile molecule are on a comparable time scale in the surface population. In the center population, the TCFs calculated by the two different methods are roughly the same, with the one computed via the initial position method decaying slightly slower on the intermediate time scale. The mixing in this case is negligible because the acetonitrile in the center population reorients much faster than it exchanges into the surface population.

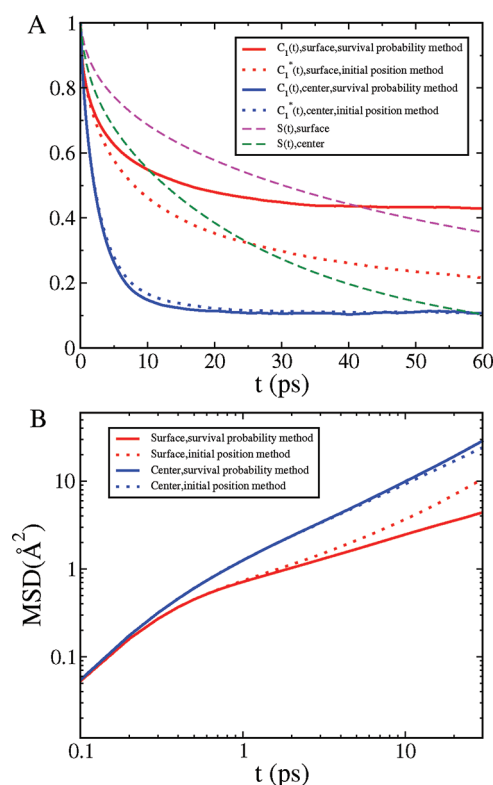


Figure 12. The dynamical properties of acetonitrile in the 24 Å OH pore calculated by two different methods. Panel A shows the singlet reorientational time correlation functions and the survival probabilities of acetonitrile in the surface population and the center population. Panel B depicts the mean square displacements in the surface population and the center population. The red and blue colors indicate the surface population and the center population, respectively. The solid and dotted lines depict the results of the survival probability and the initial position method, respectively. The dashed magenta and green lines denote the survival probabilities of the surface population and the center population, respectively.

In the initial position method, the mean square displacement along the axis of the cylindrical pore is calculated by the following equation:

$$MSD^*_{1z}(t) = \frac{1}{T} \sum_{t_0=1}^T \frac{1}{N^*(t_0)} \sum_{i \in S^*(t_0)} (Z_i(t_0 + t) - Z_i(t_0))^2 \quad (5)$$

where $N^*(t_0)$ and $S^*(t_0)$ share the same meaning as those in eq 4.

The MSDs calculated by the two different methods for the 24 Å OH pore are shown in a double logarithmic scale in Figure 12B. For the surface population, the MSDs calculated by the two different methods are the same for times less than 1 ps. For times greater than 1 ps, the MSD calculated by the initial position method deviates from the MSD of the survival probability method, with its slope increasing from 0.55 to 1. It exhibits Brownian diffusive behavior after 10 ps. The diffusion constant is $0.175 \text{ \AA}^2/\text{ps}$, if linear fitting is applied in the time window from 10 to 30 ps. However, we note that after 10 ps more than 30% of the surface population has been exchanged into the center population. Thus, when it is calculated by the initial position method, the MSD of the surface population

carries evident characteristics from the center population. Furthermore, the diffusion constant obtained is not invariant when fit in windows at later times, because the mixing of the two populations increases with time. On the other hand, the MSD of the surface population calculated by the survival probability method exhibits subdiffusive behavior for times greater than 1 ps. The power-law fitting is stable until 80 ps, after which the statistics get worse as the survival probability decays. For the center population, the MSDs calculated by the two different methods are similar and linear in time. The diffusion constants are 0.428 and $0.470 \text{ \AA}^2/\text{ps}$, for the initial position method and the survival probability method, respectively, when fit from 2 to 10 ps. The diffusion constants change to 0.371 and $0.473 \text{ \AA}^2/\text{ps}$, when fit from 10 to 20 ps. The diffusion constant decreases at later times in the initial position technique due to the fact that the mixing of the two population contaminates the results. The survival probability method does not exhibit these problems.

5. DISCUSSION AND CONCLUSION

In this Article, we carry out extensive molecular dynamics simulations to understand the structure and dynamics of liquid acetonitrile confined in a nanoscale silica pore. We develop a force field, parametrized from ab initio molecular dynamics simulations. In agreement with previous simulation studies,^{3,5,6} our structural analysis demonstrates that the acetonitrile molecules within a distance of 4.5 Å from the hydroxylated silica surface form a bilayer structure with two antiparallel oriented sublayers, where acetonitriles in the closest sublayer are ordered with the nitrogen end pointing toward the surface. This antiparallel layering effect can propagate into the center regions of the pores of radius 12 and 22 Å, and it was found that such an effect could propagate for 20 Å for acetonitriles near a flat hydroxylated crystal silica surface.⁶ Through charge density profile analysis, we show that such a long-range layering effect is mainly caused by the charge distribution on the silica surface and is not sensitive to the presence of specific hydrogen-bonding interactions, in agreement with the results of ref 3.

To better differentiate the dynamics of two inherently different populations, we adopt a different approach that takes into account the survival probability of the populations when calculating the singlet orientational time correlation functions and the mean square displacements. As compared to the initial position technique,⁷ the present method better differentiates the different populations and offers a sharper picture of the two population dynamics. For the three pore functionalizations studied, the orientational relaxation of the surface populations is constrained by the surface and decays to plateaus whose values are higher than found for the center populations. Only for the surface population in the pore that includes hydrogen-bonding interactions is the relaxation of the orientational fluctuations qualitatively different from that of the bulk acetonitrile population. In this way, specific hydrogen-bonding interactions greatly impact the dynamics at the interface. On the basis of the survival probability approach and Loughnane et al.'s work,¹ we find that the total singlet reorientational dynamics could be well reproduced with a two-population exchange model. Furthermore, we find that singlet reorientational dynamics in specific layers has very little dependence on the diameters of the pores. Such a model could be general for strongly wetting liquids in nanopores.¹

■ APPENDIX: FORCE FIELD DEVELOPMENT

One of the aims of the present work is the development of improved force fields to accurately describe the interactions of the silica surface with acetonitrile. As noted above, this interface has previously been studied utilizing potentials based on standard combining rules and by adapting parameters from silica water interfaces.^{3–6} However, the interactions present at this interface are rather subtle, and a more thorough parametrization is desirable. We have designed an interaction potential for silica acetonitrile interfaces that is consistent with the structure garnered from first-principles molecular dynamics simulation. Our potential is composed of terms arising from silica–silica, acetonitrile–acetonitrile, and interfacial interactions:

$$V = V_{\text{silica}} + V_{\text{acetonitrile}} + V_{\text{sil-acn}} \quad (6)$$

The silica term is adopted from a recent reparameterization of the BKS model²⁶ known as CHIK.²⁷ We utilize the OPLS/AA force field to treat the acetonitrile–acetonitrile interactions.¹² The surface of the silica is hydrolyzed, that is, silanol groups replace surface defects, and their treatment is included in the interfacial term. The silanol groups are treated in the following fashion. A partial charge of -0.8675 and $+0.39$ is assigned to the OH and H sites, respectively. The intramolecular structure of the silanol is treated as flexible with the parameters of the harmonic bonding and bending potentials given in Table 1.

Table 1. Intramolecular Parameters of Silanol

pair	a_0	k
OH–HY	0.9515 Å	$4.72 \times 10^5 \text{ kJ mol}^{-1} \text{ nm}^{-2}$
OH–SI	1.560 Å	$9.16 \times 10^5 \text{ kJ mol}^{-1} \text{ nm}^{-2}$
Si–OH–HY	108.5°	$300.0 \text{ kJ mol}^{-1} \text{ rad}^{-2}$
OH–Si–OH	117.0°	$300.0 \text{ kJ mol}^{-1} \text{ rad}^{-2}$

We choose an interfacial force field comprised of electrostatic and nonbonded terms, which is given by:

$$V_{\text{sil-acn}} = \sum_{i < j} \left(\frac{q_i q_j}{r_{ij}} + V_{\text{nb}}(r_{ij}) \right) \quad (7)$$

The parameters of the nonbonded potential were tuned to yield consistency with first-principles molecular dynamics trajectories described below. The atomic partial charges are chosen to be consistent with the respective bulk potentials.^{12,27} The nonbonded interactions given by V_{nb} are represented by a Lennard-Jones potential with the exception of CZ–OH for which a Buckingham form is utilized:

$$V_{\text{buckingham}} = Ae^{-Br} - C/r^6 \quad (8)$$

with parameters $A = 3.56 \times 10^3 \text{ kJ mol}^{-1}$, $B = 1.95 \text{ Å}^{-1}$, and $C = 2.09 \times 10^3 \text{ kJ mol}^{-1} \text{ Å}^{-6}$. The Lennard-Jones interactions between silicon sites and acetonitriles are taken to be small, in accord with a prior parametrization.³ The parameters for the Lennard-Jones interactions are given in Table 2.

Nonelectrostatic interactions between the silanol hydrogen and other sites are not included in the potential with the exception of an additional 12–10 hydrogen-bonding interaction,²⁸ which is utilized to describe the hydrogen bond between the NZ and H sites:

Table 2. Lennard-Jones Parameters for Silica Acetonitrile Interactions

pair	$\epsilon \text{ (kJ mol}^{-1}\text{)}$	$\sigma \text{ (Å)}$
OH–NZ	0.603	3.14
OH–CT	0.382	3.34
OH–HC	0.208	2.55
OH–OH	0.648	3.166
OX–NZ	0.629	3.35
OX–CZ	0.438	3.34
OX–CT	0.438	3.34
OX–HC	0.209	2.907
SI–NZ	0.0769	3.02
SI–CZ	0.0479	3.07
SI–CT	0.0479	3.07
SI–HC	0.0221	2.70

$$V_{\text{h-b}} = \frac{6^6}{5^5} \epsilon \left[\left(\frac{\sigma}{r} \right)^{12} - \left(\frac{\sigma}{r} \right)^{10} \right] \quad (9)$$

with parameters $\epsilon = 1.66 \text{ kJ mol}^{-1}$ and $\sigma = 1.70 \text{ Å}$. We found it necessary include this term to reproduce hydrogen bonding without resorting to increasing the magnitude of charge on the NZ or HY site, which was found to denigrate the model in other respects.

In the methylated pore, we utilize a united atom model for the methyl group with a partial charge of -0.2 and Lennard-Jones parameters $\sigma = 3.95 \text{ Å}$ and $\epsilon = 0.732 \text{ kJ/mol}$. Geometric combining rules are employed to generate the acetonitrile–methyl interactions.

As noted above, we have chosen to parametrize our potential for the interaction of acetonitrile with a hydroxylated silica surface with respect to first-principles calculations of a (smaller) system of acetonitrile confined in between two silica surfaces. To this end, we perform Born–Oppenheimer molecular dynamics simulations utilizing the QUICKSTEP module within the CP2K package.²⁹ The electronic structure is computed by means of density functional theory and a combined Gaussian basis set/plane wave approach.²⁹ A system of 30 acetonitrile molecules confined in a silica slit was simulated for 5 ps with the TZV2P basis set and for 20 ps with the smaller but more computationally efficient DZVP basis set. The Becke exchange and Lee–Yang–Parr correlation functions are employed in all first-principles computations.^{30,31} Similar treatments have been previously used to simulate bulk acetonitrile and acetonitrile at anatase surfaces.^{32,33} Although the present trajectories are too short to study dynamical properties, they may be utilized to evaluate the structure at the first layer of the interface and provide data for the fitting of our model potential. In particular, the hydrogen-bonded interaction between acetonitrile and the surface may be characterized.

In Figure 13, we compare the radial distribution functions of the heavy atoms of acetonitrile from the silanol groups garnered from the first-principles simulation with the final iteration of our force field. The radial distribution functions have been renormalized following the method in Soper et al.'s work.^{14,15} It can be seen that the simulations performed with the two basis sets are in good agreement with each other; also from the first-principles simulation, it is clear that the cyanide group accepts a hydrogen bond from the silanol. Hydrogen bonding plays a critical role in determining the nature of the interface, and reproducing such effects requires a careful balancing of electrostatic and other nonbonded interactions. Our force

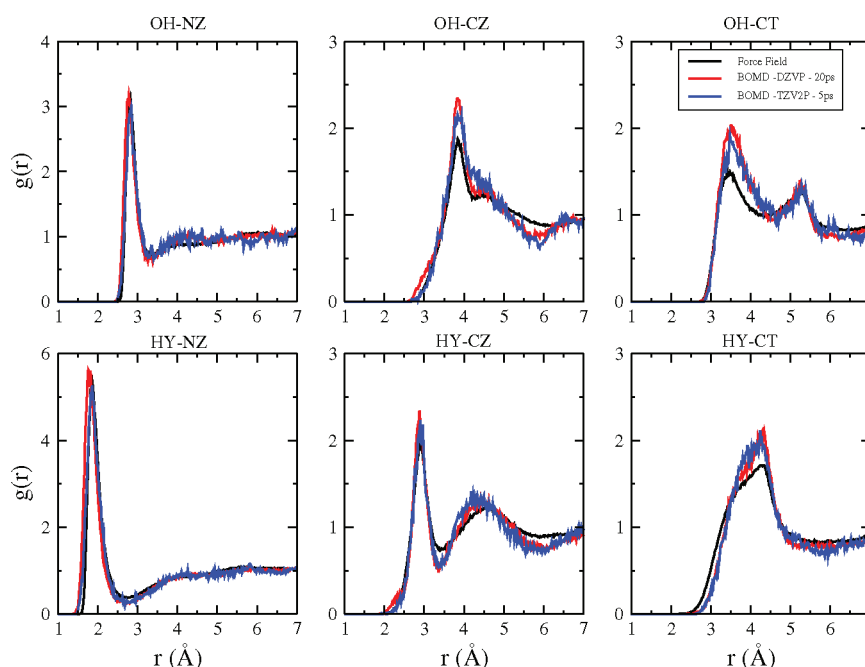


Figure 13. The renormalized radial distribution functions between atoms of the silanol group (the hydroxyl oxygen OH and the hydroxyl hydrogen HY) and the heavy atoms of acetonitrile (the cyanide nitrogen NZ, the cyanide carbon CZ, and the methyl carbon CT) in the silica slab system simulated by molecular dynamics utilizing the present force field (black), and ab initio molecular dynamics with the DZVP basis set (red) and the TZV2P basis set (blue).

field has been optimized so as to yield good agreement with these distributions, in addition to other structural properties. One finds that our force field is successful at matching the first-principles result. Furthermore, it can be seen that the OH–NZ distribution and the HY–NZ distribution sharply peak at approximately 2.8 and 1.8 Å, respectively. This is again indicative of the presence of hydrogen bonding. Further analysis indicates that, as expected, those molecules that are closest to the surface prefer to be oriented with the nitrogen pointing toward the surface. This feature is consistent with the results of prior work,^{3,5,6} and the observation that there is greater structure near the interface is consistent with all of the simulations that we have undertaken.

AUTHOR INFORMATION

Corresponding Author

*E-mail: bb8@columbia.edu.

Notes

The authors declare no competing financial interest.

ACKNOWLEDGMENTS

This research was supported by the National Science Foundation through a CRC grant (CHE 0628178). We thank Profs. John Fourkas, John Weeks, Rob Walker, and Zhonghan Hu for useful discussions about this research, and Dr. Sterling Paramore for insights springing from his early work on related problems.

REFERENCES

- (1) Loughnane, B.; Farrer, R.; Scodinu, A.; Fourkas, J. J. *Chem. Phys.* **1999**, *111*, 5116.
- (2) Horng, P.; Brindza, M. R.; Walker, R. A.; Fourkas, J. T. *J. Phys. Chem. C* **2010**, *114*, 394.
- (3) Morales, C. M.; Thompson, W. H. *J. Phys. Chem. A* **2009**, *113*, 1922.
- (4) Gulmen, T.; Thompson, W. *Langmuir* **2009**, *25*, 1103.
- (5) Hu, Z.; Weeks, J. D. *J. Phys. Chem. C* **2010**, *114*, 10202.
- (6) Ding, F.; Hu, Z.; Zhong, Q.; Manfred, K.; Gattass, R. R.; Brindza, M. R.; Fourkas, J. T.; Walker, R. A.; Weeks, J. D. *J. Phys. Chem. C* **2010**, *114*, 17651–17659.
- (7) Milischuk, A. A.; Ladanyi, B. M. *J. Chem. Phys.* **2011**, *135*, 174709.
- (8) Liu, P.; Harder, E.; Berne, B. J. *J. Phys. Chem. B* **2004**, *108*, 6595–6602.
- (9) Hess, B.; Kutzner, C.; van der Spoel, D.; Lindahl, E. *J. Chem. Theory Comput.* **2008**, *4*, 435.
- (10) Brinker, C. J.; Scherer, G. W. *Sol-Gel Science: The Physics and Chemistry of Sol-Gel Processing*; Academic: San Diego, CA, 1990.
- (11) Rodriguez, J.; Elola, M. D.; Laria, D. *J. Phys. Chem. B* **2010**, *114*, 7900–7908.
- (12) Price, M. L.; Ostrovsky, D.; Jorgensen, W. J. *Comput. Chem.* **2001**, *13*, 1340.
- (13) Liu, S.; Hu, Z.; Weeks, J. D.; Fourkas, J. T. *J. Phys. Chem. C* **2012**, *116*, 4012–4018.
- (14) Soper, A. K. *J. Phys.: Condens. Matter* **1997**, *9*, 2399.
- (15) Mancinelli, R.; Imberti, S.; Soper, A. K.; Liu, K. H.; Mou, C. Y.; Bruni, F.; Ricci, M. A. *J. Phys. Chem. B* **2009**, *113*, 16169.
- (16) *Handbook of Chemistry and Physics*, 77th ed.; Lide, D. R., Ed.; CRC Press: Boca Raton, FL, 1996.
- (17) Zhang, J.; Jonas, J. *J. Phys. Chem.* **1993**, *97*, 8812.
- (18) Loughnane, B.; Scodinu, A.; Fourkas, J. J. *J. Phys. Chem. B* **1999**, *103*, 6061.
- (19) Loughnane, B.; Farrer, R.; Fourkas, J. J. *J. Phys. Chem. B* **1998**, *102*, 5409.
- (20) Laage, D.; Thompson, W. H. *J. Chem. Phys.* **2012**, *136*, 044513.
- (21) Metzler, R.; Klafter, J. *Phys. Rep.* **2000**, *339*, 1.
- (22) Wong, I. Y.; Gardel, M. L.; Reichman, D. R.; Weeks, E. R.; Valentine, M. T.; Bausch, A. R.; Weitz, D. A. *Phys. Rev. Lett.* **2004**, *92*, 178101.
- (23) Gallo, P.; Rovere, M.; Chen, S. H. *J. Phys.: Condens. Matter* **2010**, *22*, 284102.
- (24) Gallo, P.; Rovere, M.; Spohr, E. *J. Chem. Phys.* **2000**, *113*, 11324.
- (25) Easteal, A. J. *Aust. J. Chem.* **1980**, *33*, 1667.
- (26) vanBeest, B.; Kramer, G.; Santen, R. V. *Phys. Rev. Lett.* **1990**, *64*, 1955.

- (27) Carre, A.; Horbach, J.; Ispas, S.; Kob, W. *Europhys. Lett.* **2008**, *82*, 17001.
- (28) Weiner, S. J.; Kollman, P. A.; Case, D. A.; Singh, U. C.; Ghio, C.; Alagona, G.; Profeta, S.; Weiner, P. *J. Am. Chem. Soc.* **1984**, *106*, 765.
- (29) VandeVondele, J.; Krack, M.; Mohamen, F.; Parrinello, M.; Chassaing, T.; Hutter, J. *Comput. Phys. Commun.* **2005**, *167*, 103.
- (30) Becke, A. *Phys. Rev. A* **1988**, *38*, 3098.
- (31) Lee, C.; Wang, W.; Parr, R. *Phys. Rev. B* **1988**, *37*, 785.
- (32) VandeVondele, J.; Lynden-Bell, R.; Meijer, E. J.; Sprik, M. *J. Phys. Chem. B* **2006**, *110*, 3614.
- (33) Schiffmann, F.; Hutter, J.; VandeVondele, J. *J. Phys.: Condens. Matter* **2008**, *20*, 064206.